Scanning Electric Potential Microscopy Imaging of Polymer Latex Films: Detection of Supramolecular Domains with Nonuniform Electrical Characteristics

Melissa Braga, Carlos Alberto Rodrigues Costa, Carlos Alberto Paula Leite, and Fernando Galembeck*

Instituto de Química, Universidade Estadual de Campinas, P.O. Box 6154, 13083-970 Campinas SP, Brazil

Received: July 26, 2000; In Final Form: November 13, 2000

Scanning electric potential microscopy (SEPM) together with noncontact AFM images were obtained from the surfaces of two latex films: the first is a self-arrayed poly(styrene-*co*-hydroxyethyl methacrylate) macrocrystal, while the other is a thin film formed by coagulation of polystyrene particles at the latex liquid surface, under exposure to chloroform vapor. In both cases, large electric potential differences are detected by the microscope probe between adjacent domains in the films. Domains with positive or negative potentials reach a few hundred nanometers in size. These dielectric films are thus mosaics of electrically charged domains, and their electroneutrality is only observed at the macroscopic level.

Introduction

Polymer latex particles usually contain ionic groups, originated from initiator residues, surfactant, and counterions.[1] The fate of these ions when the particles coagulate or they are transformed into films is an interesting problem, due to their effect on the polymer solid properties. There are two major possibilities: ions can exudate to the polymer surface, which was demonstrated in the case of surfactants,[2] or they are incorporated within the polymer bulk, which is certainly a poor solvent for ionic compounds. It is not possible to have a complete ion exudation to the surface, since at least part of the ionic groups are covalently bound to the polymer chains and these are much smaller than the macroscopic solid or film dimensions. The residual ions should have an important role in the modification of the polymer properties, either imparting ionomeric[3] properties to it or contributing to an enhanced water sorption ability and consequently to its permeability and electrical properties.

It is then desirable to detect and to identify the distribution of ions within thermoplastics or rubbers made out of latex. This was recently done for the first time, when the elemental maps of poly(styrene-*co*-hydroxyethyl methacrylate) (PS−HEMA) latex particles obtained by electron energy loss spectroscopy (EELS) coupled to transmission electron microscopy were published.[4−6] These maps revealed a rather unexpected and nonuniform pattern for sulfur (from sulfate) and potassium counterions distribution throughout the dry latex particles: sulfate is more concentrated at the particles interior than at their surfaces, while potassium ions are within an outer thick shell. However, both in smaller PS−HEMA particles and in homopolymeric polystyrene (PS) latex, both sulfate and potassium ions were found distributed throughout the particles.[7] These results lead to two conclusions: first, there is not a single pattern for charge distribution within latexes; second, dry latex particles are electroneutral, but ions carrying electrical charges of the same signal are clustered in domains extending for tens or hundreds of nanometers.

The advent of the scanning probe microscopes made available techniques for sensing or measuring charges, dielectric constants, film thickness of insulating layers, and photovoltage and electric potentials,[8] as well as for ferroelectric domain imaging.[9] These techniques allow us to circumvent the well-known difficulties for the direct measurement of electric potentials in dielectrics in a way analogous to the techniques devised for monolayer electric potential measurement.[10] For instance, the scanning electric potential and electrostatic force microscopes (SEPM and EFM) map the spatial variation and potential energy difference between a tip and a sample, arising from nonuniform charge distributions[11] as well as from variations in the surface work function.[12] Another example is a tapping mode atomic force microscope (AFM) coupled to electrostatic force modulation, which was used to image a polystyrene latex layer deposited on silicon, showing a large and intriguing contrast between neighboring latex particles.[13] Localized charges on polymers were imaged by Terris et al.,[14] using PMMA samples carrying charges implanted by ion bombardment.

In this work, we report SEPM images of a coalesced polystyrene latex thin film, obtained by surface coagulation induced by solvent vapor.[15] This sample is specially interesting, because it presents two different surfaces (one formed in contact with air, the other formed in contact with water) of a thin film, obtained without using any mechanical means, thus avoiding tribochemical effects. We present also SEPM images of a dry poly(styrene-*co*-hydroxyethyl methacrylate) latex film, for which elemental maps obtained by energy loss imaging in the transmission electron microscope (ESI-TEM) are available,[4] thus allowing us to establish a correlation between the microchemical information and the electric potential maps.

Experimental Procedure

Polystyrene latexes, PS−M and PS−HEMA were prepared in this laboratory. PS-M is a homopolymer latex, prepared and characterized in a previous work,[16] using Brij 35 and SDS as emulsifiers and potassium persulfate as the initiator. PS−HEMA is a poly(styrene-*co*-2-hydroxyethyl methacrylate) latex, prepared following the methods of Tamai et al.[17] and Kamei et

* To whom correspondence should be addressed.

10.1021/jp002667d CCC: $20.00
Published on Web 03/28/2001

al.[18] Polymerization is initiated by $K_2S_2O_8$, in the absence of surfactant. The yield was 94% with a 14.3% solids content.[19] In every case, the amount of coagulated material was less than 1%.

Both latexes were filtered with a 200 mesh steel sieve to remove coagulated latex. To remove excess emulsifiers, unreacted monomer, and unwanted electrolyte, the samples were subsequently dialyzed against water with daily changes over a 1-month period, until the conductivity of the dialysate reached 4 μS/cm and remained unchanged for 48 h. After dialysis, the samples were dispersed in water as required for reaching the desired concentrations.

Particle size and ζ potential determinations were performed in a Brookhaven ZetaPlus instrument. To achieve adequate signal intensity, a 0.1 mL stock latex dispersion was diluted with 2 mL of water (for particle sizes) or 10^{-3} M KCl solution (for ζ potential). Palladium electrodes were used. Effective diameters of PS−HEMA and PS−M latex particles are respectively 427 and 100 nm, and the zeta potentials are −41 and −28 mV.

Film preparation was done as follows: 1−1.5 mL of PS−M latex (2% w/w solids content) was placed within a 15 mL glass vial together with another vial containing 3 mL of chloroform, both within a closed glass container in a room at 25 ± 2 °C. After a 1-week exposure, a film was formed at the latex surface and it became strong enough to be collected over a thin Nichrome wire ring, after 2 weeks. The ring was first immersed in the liquid, placed beneath the film and moved upward.

The PS HEMA latex film was obtained by sedimentation and drying in a Petri dish within a desiccator at 25 °C, using an aliquot of the opalescent bottom fraction of a settled PS−HEMA dispersion. The detailed description of the film preparation and film morphology are given elsewhere.[18]

Atomic force (AFM) and electric potential (SEPM) microscopy experiments were performed simultaneously in a Topometrix Discoverer instrument; images of the two types were obtained from the same area, at the same time.

The noncontact AFM mode was used to obtain topographic information on the latex films. This technique has been widely used, and a detailed description is thus unnecessary. Topography changes were sensed by monitoring detector signal amplitude at 300 × 300 pixel resolution and 1.81 μm/s scan rate, using Pt-coated Si tips with a 20-nm nominal radius, which was verified by imaging a tip in a JEOL JSM-6340F high-resolution scanning electron microscope.

In this instrument, SEPM uses the standard noncontact AFM setup, but with the following modifications: the Pt-coated conducting tip is fed with a 5 V ac signal, 10 kHz below the frequency of the normal AFM oscillator, which matches the natural frequency of mechanical oscillation of the cantilever-tip system (40−70 kHz). During a measurement, the mechanical oscillation of the tip is tracked by the four-quadrant photodetector and analyzed by two feedback loops. The first loop is used in the conventional way to control the distance between tip and sample surface (10 nm), while the sample is scanned at constant oscillation amplitude. The second loop is used to minimize the changes of the electric field between tip and sample: the second lock-in amplifier measures the ac frequency oscillation while scanning and adds a dc bias to the tip, to recover the undisturbed ac oscillation. The principle is analogous to the Kelvin method, except that forces are measured instead of currents.[8,19] This technique differs from that used by Terris,[13] who measured the phase displacement of the ac voltage, while in the Topometrix set up we cancel the phase displacement by dc biasing. The image is built using the dc voltage fed to the tip, at every pixel, thus detecting electric potential gradients throughout the scanned area. This technique is reminiscent of the oscillating electrode technique[20] for monolayer study: both use an oscillating electrode separated from the sample by an air gap. The major difference between them is the detection technique used, since SEPM uses a phase detection of the perturbations on the applied ac voltage.

SEPM technique has a good lateral resolution, as compared to other electric mapping techniques, because the sample to tip distance is kept at 10 nm only, while the methods based on electric force measurements depend on scanning at 40 nm or more. A detailed study of the errors introduced by scanning at different heights was published by Hong et al.,[21] showing that the electric fields measured by a scanning probe 10 nm above the surface at lateral distances larger than 100 nm from the source are affected by errors lower than 10%; for shorter lateral distances, the errors may be as large as 30%, but the field polarity is always correct.

Image processing was performed by a PC microcomputer using Image-Pro Plus 4.0 (Media Cybernetics) as well as the Topometrix image analysis program.

Transmission Electron Microscopy (TEM) and Elemental Spectroscopy Imaging (ESI). Bright-field pictures and the elemental distribution within latex particles were obtained using a Carl Zeiss CEM-902 transmission electron microscope, equipped with a Castaing-Henry-Ottensmeyer energy filter spectrometer within the column. When the electron beam passes through the sample, interaction with electrons of different elements results in characteristic energy losses. A magnetic prism−mirror system deflects electrons with different energies to different angles so that only those electrons with a well-defined energy are selected. If elastic electrons only are chosen ($\Delta E = 0$ eV), a transmission image with reduced chromatic aberration is obtained. When monochromatic inelastically scattered electrons are selected, electron spectroscopic images (ESI) are formed, in which contrast is dependent on the local concentration fluctuations of a particular chosen element. Clear areas correspond to element-rich domains.

For the examination of latex particle submonolayers, one drop of the latex dispersion (1% solids content) was deposited on carbon-coated parlodion films supported in 300 mesh copper grids (Ted Pella). To make sure that the particles were not excessively thick, they were first observed using $\Delta E = 0$ eV (elastic scattered monochromatic electrons) and then observed again at $\Delta E = 20-50$ eV. Image contrast inversion was always obtained, showing that a significant number of electrons were transmitted throughout the particles.[23] This observation is understood, considering that the 80 keV electrons mean free path within these latex particles is greater than 160 nm for elastic scattering[24] and is estimated as many hundreds of nanometers, for inelastic scattering.

Elemental images were obtained for the relevant elements found in this sample, using monochromatic electrons corresponding to the carbon K-edge, oxygen K-edge, sulfur L_3-edge, potassium L_3-edge, and sodium L_3-edge, with an energy-selecting slit of 15 eV. The images were recorded by a Proscan high-speed slow-scan CCD camera and processed by the AnalySis 3.0 system.

Results

Figure 1 presents AFM and SEPM images of a PS−HEMA latex dry film surface. These are used to verify the results obtained by SEPM, because the distribution of ionic groups in

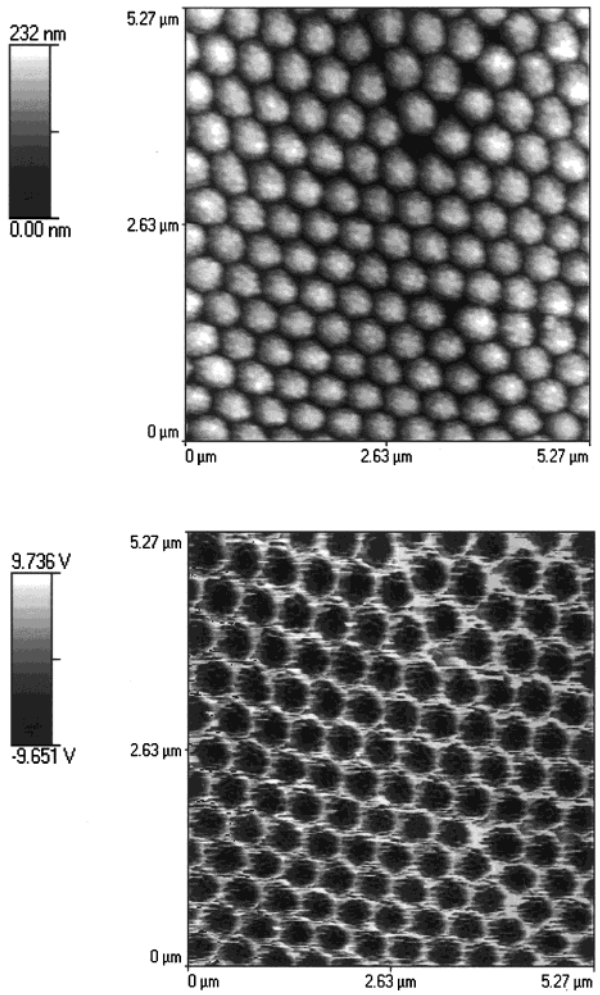

Figure 1. AFM (top) and SEPM (bottom) images of a self-assembled poly(styrene-*co*-hydroxyethyl methacrylate) latex macrocrystal. Particles have a "raspberry" morphology, and according to EELS microanalysis, the negatively charged sulfate groups are in the interior of the particles and the potassium counterions are clustered at the particle surfaces.[4]

this latex is well-known. The particle central areas are predominantly negative relative to the interparticle spaces, but there are also small positive domains dispersed over the particle central areas. This is consistent with the microchemical data obtained by ESI-TEM, according to which the negative sulfate ions predominate in the particle interior and potassium cations are concentrated at the particle borders, in the dry particle film.[4]

A bright-field electron transmission micrograph and the corresponding elemental maps of PS-M particles are shown in Figure 2. From the observation of these images, we can draw the following conclusions:

(i) The particles appear evenly dark, in the bright-field picture. They are not coalesced, but necking is observed in the zoomed images (not shown). A few particles are piled up on top of others, but the respective contours are distinct.

(ii) Neighboring particle brightness is rather uniform in the C map, as expected considering that particle sizes are uniform and this is a homopolymer latex.

(iii) Particle brightness is also uniform in the Na and K maps, showing that these counterions are evenly sorbed within the particles.

(iv) The S map is quite different from all the previous ones. First, the particles appear smaller than in the other maps; consequently, this element is concentrated in the particle cores and it is depleted in the shells, following a pattern observed in other latexes.[4,7] Second, the brightness level of different particles is quite variable, showing (by comparison to the C map) that the particles have large variations in the S/C content ratio. This implies necessarily a large variation in the PS molecular weights.

(v) The O map is similar to the S map, but the apparent particle diameters appear larger in the former. Part of the oxygen in the particles is associated with S, since the two elements are together in the sulfate ions. However, there is also a contribution to the oxygen map made by hydroxylated chain ends (from sulfate hydrolysis) as well as by the water sorbed by the particles, even under the microscope high vacuum. This is verified by concentrating the electron beam over the particles, when these are heated. Then, both the bright-field image and the O map are modified, which is assigned to the loss of sorbed water.

Topography and SEPM images of the coalesced PS latex film's upper side, formed in contact with the chloroform-saturated atmosphere, are in Figure 3. The surface is very flat, with elevations and depressions that are not uniformly correlated to the electrical features seen in the electric potential map. For instance, the elevation close to the image center is made out of at least four electrically distinguishable domains, out of which two are negative (dark), one (in the particle center) is intermediate, and a surrounding rim is positive (bright). A histogram of the pixel gray levels of the two images is in Figure 4, showing the strong mismatch between the distribution of heights and electric potentials.

Line scans were obtained from both images in Figure 3, across the two pairs of horizontal lines superimposed to the images, and they are shown in Figure 5. The lack of correlation between the two pairs of curves is evident, concerning both the larger as well as the smaller image features.

Large electric potential gradients are estimated by reading the electric potential differences across adjacent areas, e.g. around the higher elevation in this field. The potential differences reach a few volts, between pixels that are just 50 nm apart. This means that the microscopic observed gradients are in the 10^7−10^8 V/m range, which is the same as that for the macroscopically measured dielectric strength for polystyrene.[25]

The film's lower surface (which is formed in contact with liquid) was also observed in samples taken from the latex surface and dried without rinsing, and the images are shown in Figure 6. From the AFM image, we see that this surface is very rough, containing a large number of distinguishable, poorly coalesced particles. The SEPM picture shows bright (positive) lines surrounding many particles, as well as a large number of darker spots, smaller than the particles and thus showing a clustering of negatively charged groups. We note that small dark spots in the same size range are also seen in the SEPM image in Figure 3.

The sharp contrast at the particle borders in the SEPM image but not in AFM (Figure 6), is easily understood if we consider that countercations from the diffuse double-layer in the latex serum should accumulate at the drying particle surfaces, the same as in the case of the PS−HEMA latex (Figure 1).

Discussion

The large contrast observed in the image of the PS−HEMA latex can be easily understood, considering the known microchemical features of this system. When the tip scans the lateral domains of adjacent particles it senses an excess positive (K^+) charge, as opposed to the particle centers richer in sulfate end

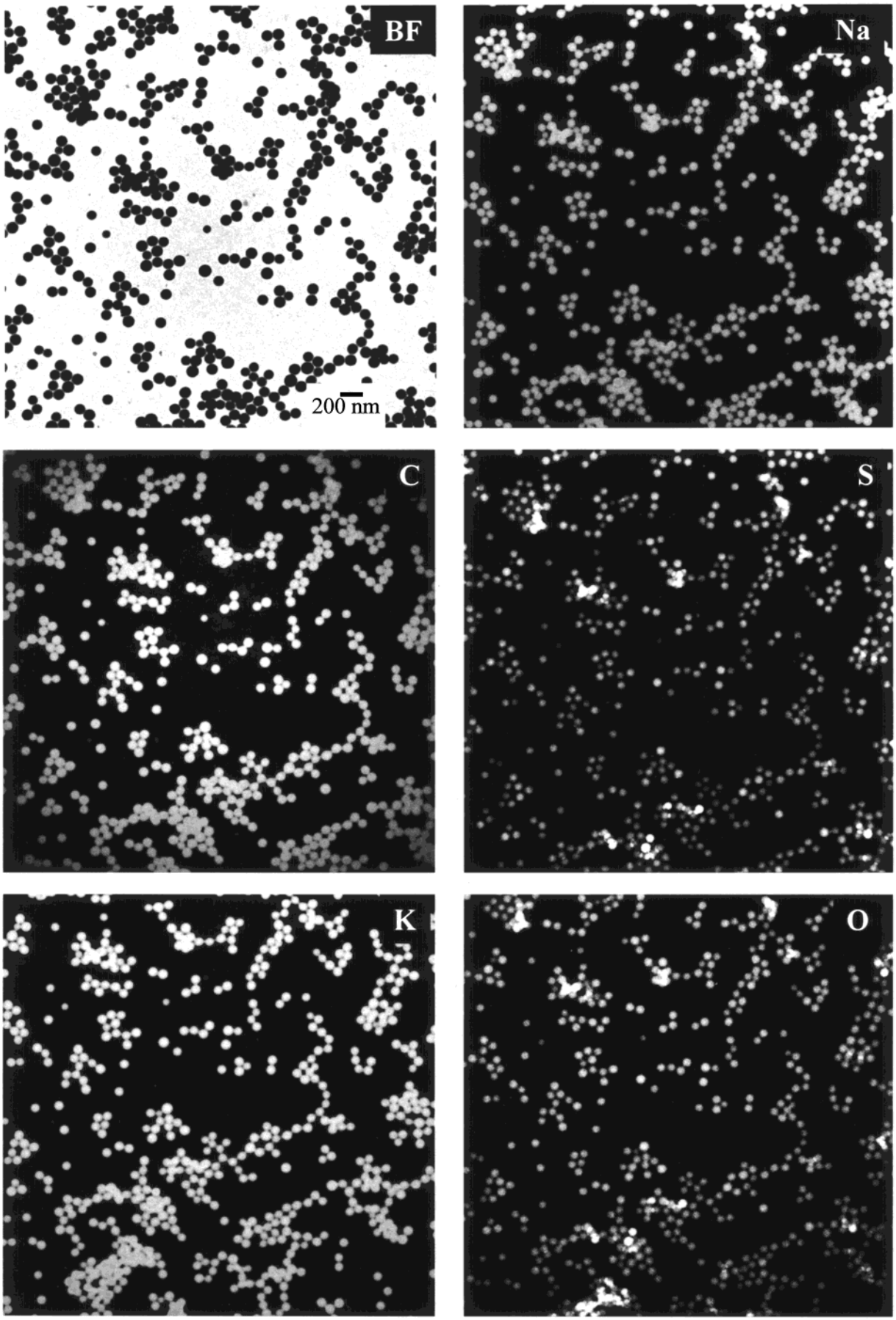

Figure 2. Bright-field electron transmission image (BF) of PS−M and elemental maps of the same field, obtained by energy-loss spectroscopy imaging (ESI) for the elements sodium, potassium, carbon, sulfur, and oxygen.

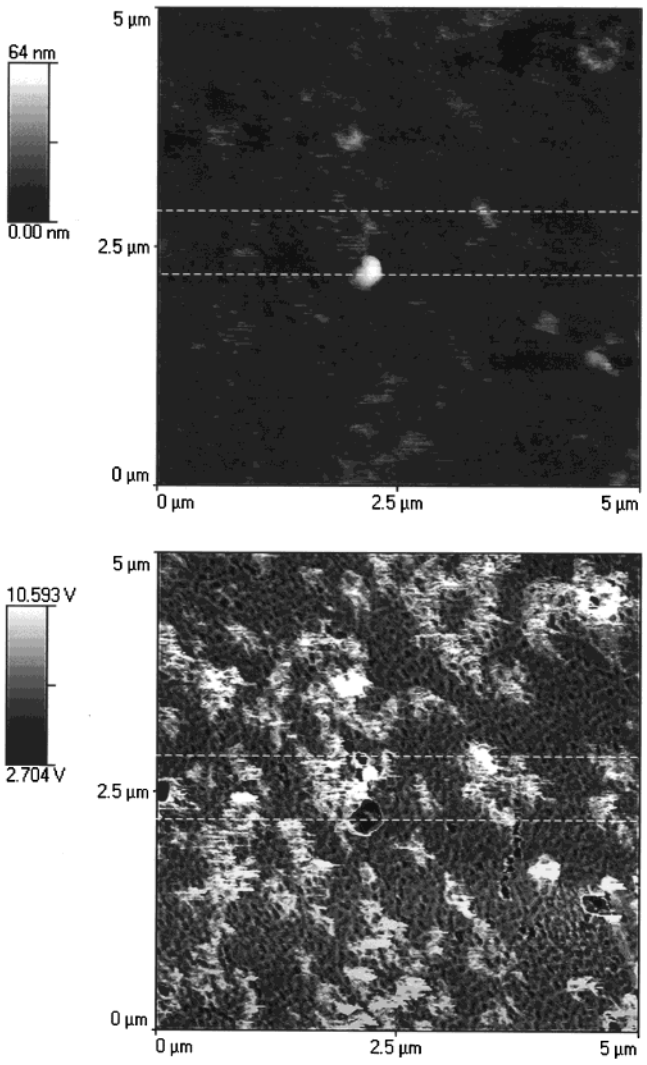

Figure 3. Noncontact AFM (top) and SEPM (bottom) images of PS−M latex film formed by surface coagulation, under chloroform vapor (surface formed in contact with air). The horizontal lines (---) indicate the positions at which gray levels were measured. The corresponding line scans are plotted in Figure 5.

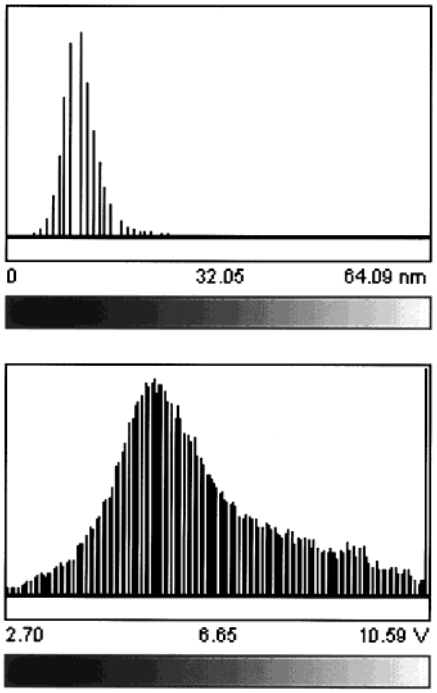

Figure 4. Histogram of the pixel gray levels of the images in Figure 3, showing the frequency of the distribution of height and electric potentials in the sample. The frequencies are on the *y*-axis, in a linear scale.

groups that are residues of the persulfate initiator. Electric potential gradients in the coalesced PS latex film are smaller than in PS−HEMA, but still important. These gradients of electric potentials (ca. 10^8 V/m) are remarkable, particularly considering that these are solid dielectric polymer films, in which the existence of electrically charged domains is usually disregarded. However, we note that the observed potential gradients are due to fixed, ionic charges without a possibility for electron injection, as in the measurement of dielectric strengths.

Since the positive or negative domains extend for hundreds of nanometers, electroneutrality is observed, but only at a supramolecular scale, rather than at a macromolecular or ion-sized scale, which is the currently usual assumption for most solids.[26] We do not advance any detailed explanation for the existence of these charge clusters, but a clue is perhaps in the ideas put forward by DeGennes,[27] Khoklov,[3] and other authors to explain macromolecular cluster formation in some systems, even when the pair interactions are completely repulsive.

SEPM contrast is much sharper in the very thin and nanometrically flat PS film than in some film regions covered by thick particles. This leads to the following conclusion: electrically contrasting domains are superimposed perpendicularly to the scanned surface, so that the tip will sense the result of a summation of opposite charges, producing images with extensive areas with a low contrast, as seen in Figure 6. For a randomly assembled thick sample, this sum will always tend to zero, thus making the usually electroneutral solids (but with many important and well-known exceptions, such as the electrets). On the other hand, the sides of large uncoalesced particles still show markedly positive domains, due to the countercation accumulation at the particle surfaces.

The presence of mobile electrical charges in dielectrics is always to be expected,[28] but we have little information on their nature in most cases. On the other hand, the images presented in this work bear a resemblance to the schematic view put forward by Wu et al.[26] concerning the contiguity of ions of opposite charges in polymers. These authors examined hydronium ions deposited at a methylpentane−water interface, and they showed that the migration of the ions into the hydrocarbon is strongly dependent on the amount of water contacting the interface. Consequently, contiguous charged clusters may be formed at interfaces, and they are partitioned according to the nature of the contacting phases.

In an earlier work, Martin and colleagues[29] observed that the force on a tip scanning over a photoresist film was much more irregular than when the tip scanned the silicon wafer under the resist. The authors did not further discuss this, and we can now interpret their observation as evidence of the presence of electrically charged domains, in the resist film.

As in all other cases of scanning force microscopies, the interpretation of the SEPM images is not straightforward, and it will depend on the progress in image simulation. Modeling of noncontact scanning force microscopy on ionic surfaces and calculations combining the effects of van der Waals and electrostatic interactions have been done recently, but only in very simple cases.[30] This will probably soon help in the interpretation of the experimental images of complex materials.

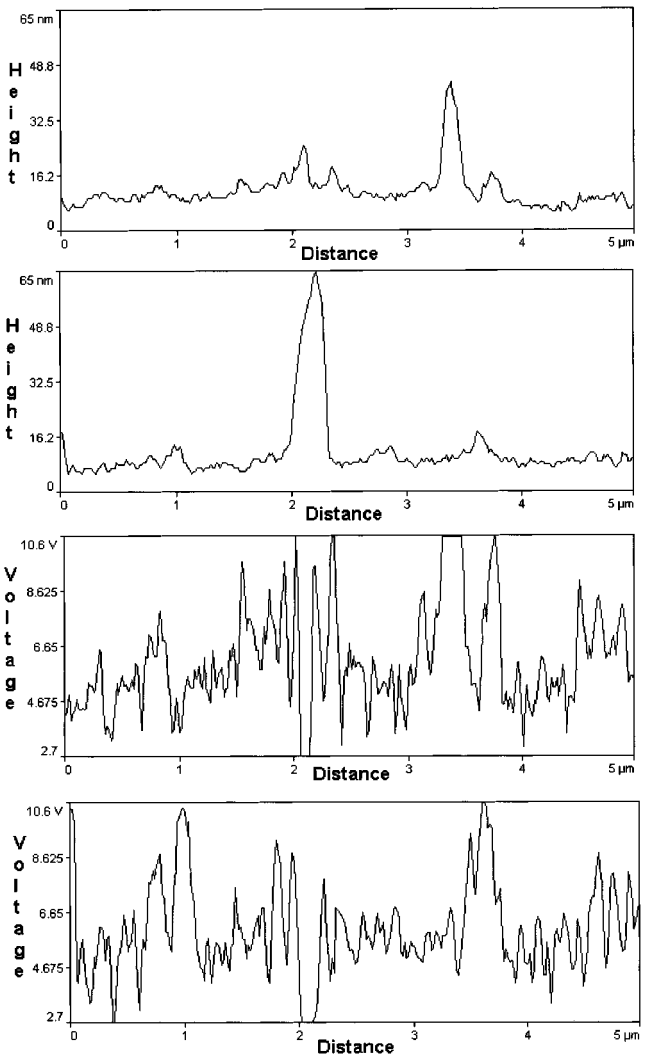

Figure 5. Horizontal line scans obtained from two positions in the AFM and SEPM images in Figure 3. Contrast in SEPM is sharper, and differentiated domains are smaller than in AFM.

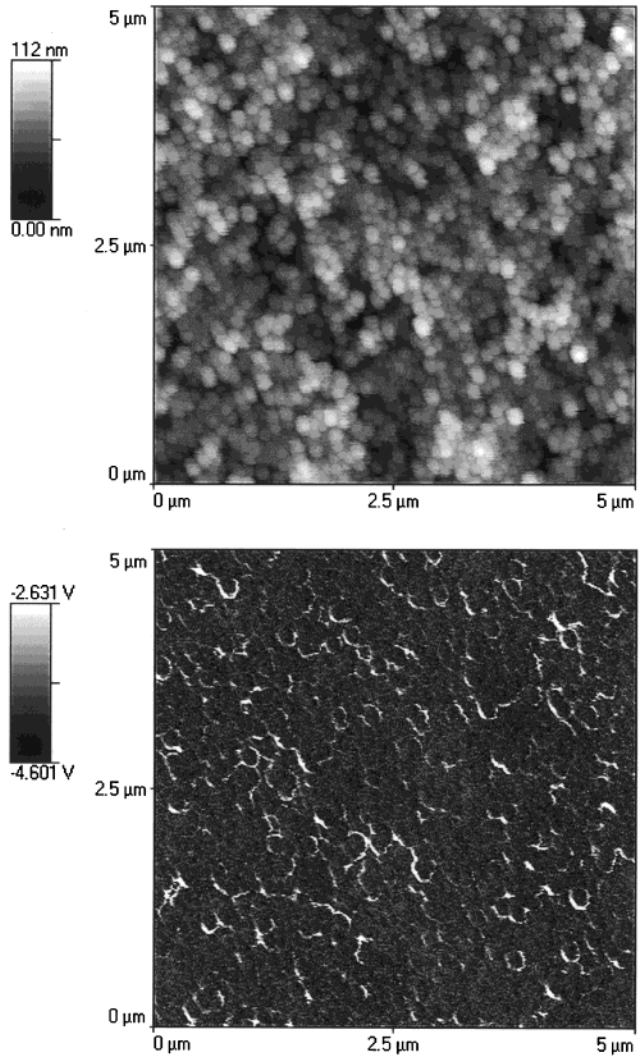

Figure 6. AFM (top) and SEPM (bottom) images of the PS−M film surface formed in contact with the liquid and rinsed prior to drying.

The present observations create at once an opportunity and some challenges. The opportunity is the use of the knowledge on charged domains to improve the mechanical, electrical, and other properties of the solids made out of dry latex. One challenge is to understand the mechanism for the formation as well as the unexpected stability of the large ionic clusters responsible for the observed electric potential gradients. Another question concerns the nature of the electrically contrasting domains. Besides the contribution of sulfate initiator residues and countercations, we cannot completely neglect the possibility for tribochemical[31] charge deposition, originated from the mechanical tensions developed during film formation.

To sum up, the results presented in this work reveal a rich nanometric mosaic of electric potentials in rather usual latex films. This is interesting from many points of view. First, an additional technique is available for polymer surface imaging; second, the images obtained depart from the prevailing electroneutral pictures for these systems. Third, this may provide relevant and currently scarce information on the electrical properties of latex films and other dielectric materials, as well as on the nature of the charge-bearing species.

We plan to present more detailed reports on specific model systems soon, as well as on other dielectric solids. However, the present results already show unexpected new information on the electrical structuring of otherwise well-known systems.

Conclusions

SEPM images of latex films are independent of the topography images evidencing the good separation of electric and van der Waals contributions to image formation. Electric potential distribution across the polymer films reveals the existence of domains of different charge densities, extending for a few nanometers up to hundreds of nanometers. Film electroneutrality is thus a result of charge balance but on a supramolecular or colloidal size scale, well beyond the size scale of ion pairs or ion clusters.

Acknowledgment. CNPq, Fapesp, and Pronex/Finep/MCT supported this work.

References and Notes

(1) Buscall, R.; Ottewill, R. H. *Polymer Colloids*, Elsevier: London, 1985; Chapter 5.

(2) Niu, B.-J.; Urban, M. V. *J. Appl. Polym. Sci.* **1996**, *60*, 389.

(3) Khokhlov, A. R.; Kramarenko, E. Y. *Macromolecules* **1996**, *29*, 681.

(4) Cardoso, A. H.; Leite, C. A. P.; Galembeck, F. *Langmuir* **1998**, *14*, 3187.

(5) Cardoso, A. H.; Leite, C. A. P.; Galembeck, F. *Langmuir* **1999**, *15*, 4447.

(6) Cardoso, A. H.; Leite, C. A. P.; Galembeck, F. *J. Braz. Chem. Soc.* **1999**, *10*, 497.

(7) Amalvy, J. I.; Asua, J. M.; Leite, C. A. P.; Galembeck, F. *Polymer* **2001**, *42*, 2479.

(8) Nonnenmacher, M.; O'Boyle, M. P.; Wickramasinghe, H. K. *Appl. Phys. Lett*. **1991**, *58*, 2921.

(9) Bluhm, H.; Wadas, A.; Wiesendanger, R.; Meyer, K.-P.; Szczesniak, L. *Phys. Rev. B* **1997**, *55*, 4.

(10) Saurenbach, F.; Terris B. D. *Appl. Phys. Lett*. **1990**, *56*, 1703.

(11) Adamson, A. W. *Physical Chemistry of Surfaces*, 5th. ed.; Wiley: New York, 1990; Chapter 3.

(12) Nyffenegger, R. M.; Penner, R. M.; Schierle, R. *Appl. Phys. Lett.* **1997**, *71*, 1878.

(13) Wong, J. H.; Khim, Z. G.; Sou, A. S.; Park, S. *Appl. Phys. Lett.* **1996**, *69*, 2831.

(14) Terris, B. D.; Stern, J. E.; Rugar, D.; Mamin, H. J. *J. Vac. Sci. Technol. A* **1990**, *8*, 374.

(15) Braga, M.; Silva, M. C. V. M.; Cardoso, A. H.; Galembeck, F. *J. Colloid Interface Sci.* **2000**, *228*, 171.

(16) Moita-Neto, J. M.; Monteiro, V. A. R.; Galembeck, F. *Colloids Surf. A* **1996**, *108*, 83.

(17) Tamai, H.; Fujji, A.; Suzawa, T. *J. Colloid Interface Sci.* **1987**, *116*, 37.

(18) Kamei, S.; Okubo, M.; Matsumoto, T. *J. Polym. Sci., Polym. Chem. Ed.* **1986**, *24*, 3109.

(19) Cardoso, A. H.; Leite, C. A. P.; Galembeck, F. *Colloids Surf. A* **1998**, *144*, 207.

(20) Weaver, J. M. R.; Abraham, D. W. *J. Vac. Sci. Technol. B*, 9, **1991**, *3*, 1559.

(21) Shaw, D. J, *Introduction to Colloid and Surface Chemistry*, Butterworth: London, 1996.

(22) Hong, J. W.; Park, S.; Khim, Z. G. *Rev. Sci. Instrum.* **1999**, *70*, 1735.

(23) We are grateful to Dr. W. Probst (LEO-Zeiss Elektronenmikroskopie Gmbh) for this valuable private communication.

(24) Newbury, D. E. In *Principles of Analytical Electron Microscopy* (Joy, D. C., Romig, A. D., Jr., Goldstein, J. I., Eds; Plenum Press: New York, 1986.

(25) Rodriguez, F. *Principles of Polymer Systems*, 2nd ed.; McGraw-Hill Book Co.: New York, 1982.

(26) Wu, K.; Iedema, M. J.; Cowin, J. P. *Science* **1999**, *286*, 2482.

(27) De Gennes, P. G. *C. R. Acad. Sci.: Paris* **1991**; *t 313*, 1117.

(28) Robert, P. *Electrical and Magnetic Properties of Materials*, Artech House: Norwood, 1988; p 300.

(29) Martin, Y.; Williams, C. C.; Wickramasinghe, H. K. *J. Appl. Phys.* **1987**, *61*, 4723.

(30) Livshits, A. I.; Shluger, A. L.; Rohl, A. L.; Foster, A. S. *Phys. Rev. B* **1999**, *59*, 2436.

(31) Heinicke, G. *Tribochemistry*; Hanser: Berlin, 1984; Chapter 3.